

Formation of Self-Assembled Quantum Wires during Epitaxial Growth of Strained GeSn Alloys on Ge(100): Trench Excavation by Migrating Sn Islands

X. Deng, B.-K. Yang, S. A. Hackney, and M. Krishnamurthy*

Department of Metallurgical and Materials Engineering, Michigan Technological University, Houghton, Michigan 49931

D. R. M. Williams

Department of Physics, Faculties and Department of Applied Mathematics, The Australian National University, Canberra, Australia 0200

(Received 18 August 1997)

A pattern of trenches and wires oriented along $\langle 100 \rangle$ directions was formed during epitaxial growth of GeSn alloys on Ge(100). The trenches appear as self-avoiding random walks at low densities and become organized into domains at higher densities. These patterns are believed to be caused by the migration of Sn islands on the surface, induced by diffusion of Ge from one side of the Sn island to the other. This morphological evolution is thought to be a kinetic pathway for phase separation of strained thin films and may be utilized for high-throughput creation of nanoscale patterns. [S0031-9007(97)05188-0]

PACS numbers: 68.55.Jk, 81.15.Hi

Epitaxial growth from the vapor is typically a far-from-equilibrium process (kinetically controlled), where most atoms arriving at the surface are incorporated within the film. By controlling the degree of adatom mobility, highly metastable films can be “quenched-in.” Examples include the growth of highly supersaturated alloys [1], or strained films grown to thicknesses beyond the equilibrium critical thickness for dislocation formation [2]. However, under the specific conditions of adatom kinetics (e.g., deposition rate, substrate temperature), the film attempts to minimize its free energy by undergoing a variety of morphological or compositional modifications [3–7].

In this paper, we report our findings and initial interpretations of the morphological evolution of an epitaxially strained Ge-Sn alloy thin film which is also metastable relative to its equilibrium composition. While phase separation appears to be the primary driving force, the presence of epitaxial strain influences the kinetic pathway and leads to the formation of an intriguing microstructural pattern of trenches and wires, apparently created by migrating Sn islands on the growing surface. Apart from being an interesting thin-film phenomenon, our observations are of much broader scientific interest. First, we find that at low trench densities the trenches form a series of self-avoiding random walks. Such walks have long been of interest to the more general scientific community, particularly in polymer science. Our system represents an experimental method of generating such walks. At higher trench densities the trenches self-organize into parallel regions, much like directed nematic polymers. Second, we believe our system represents a variant of free-energy driven droplet motion, a field of current active interest. Finally, this kinetic pathway of phase separation may offer a high-throughput technique for fabricating novel nanostructures.

Experiments were performed in a Riber molecular beam epitaxy (MBE) system with base pressure $\sim 5 \times$

10^{-10} mbar. Germanium (100) wafers were thoroughly rinsed in acetone, methanol, and deionized water to remove surface contaminants. The Ge samples were In-bonded onto a Mo substrate holder and then loaded into the MBE chamber. After outgassing at $\sim 200^\circ\text{C}$, samples were heated to $\sim 550^\circ\text{C}$ to decompose the oxide layer, following which a Ge buffer layer (20–30 nm thick) was deposited at a substrate temperature of $\sim 250^\circ\text{C}$. Both Ge and Sn were deposited from pyrolytic boron nitride Knudsen sources calibrated to have rates of ~ 0.9 nm/min for Ge and ~ 0.05 nm/min for Sn. The substrate temperature during deposition was maintained at $\sim 150^\circ\text{C}$ (estimated error $\pm 25^\circ\text{C}$). The samples had a nominal composition of 5 at. % Sn and various thicknesses between 15–60 nm. One film (~ 15 nm thick) was annealed *in situ* at 150°C for 17 h immediately after growth. All samples were analyzed *ex situ* using atomic force microscopy (AFM) (Nanoscope IIIa; Digital Instruments). Selected samples were analyzed by plan-view and cross-sectional transmission electron microscopy (TEM) using JEOL 100cx and 4000fx microscopes.

Subsequent to the growth of the Ge buffer layer, the surface showed a sharp (2×1) reconstruction pattern as observed by reflection high energy electron diffraction (RHEED). Within a few monolayers of Ge-Sn deposition, the surface reconstruction changed to a (1×1) pattern, accompanied by broadening and appearance of extra streaks which remained unchanged for the duration of the growth.

Figure 1(a) shows an AFM image of the surface morphology after codeposition of ~ 15 nm of the Ge-Sn alloy. A high density of naturally formed trenches and ridges running predominantly along crystallographic $\langle 100 \rangle$ directions is observed. Figure 1(b) shows a magnified view of a typical trench. Each trench has a rounded island at each end, a large one and a smaller one. These trenches are of

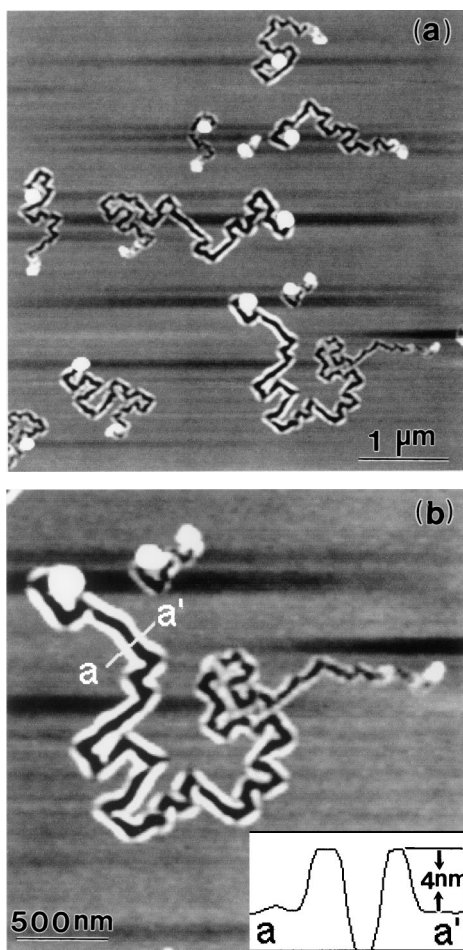


FIG. 1. (a) AFM image ($5 \mu\text{m} \times 5 \mu\text{m}$, height mode) showing a distribution of trenches and ridges on the surface of an as-grown GeSn alloy. Notice an island at each end of the trench. (b) Magnified view ($2.5 \mu\text{m} \times 2.5 \mu\text{m}$) of a typical trench and an inset showing a line-scan profile $a-a'$ across the trench and ridges.

various lengths but the widths are typically ~ 100 nm. The track width decreases gradually from the end with the large island towards the end with the smaller island. The inset shows a profile across the ridge and trench along the line $a-a'$. The trenches are typically 2–8 nm deep while the ridges are 1–4 nm high, both measured from the average surface. In general, the volume of the trench is similar to the volume of the ridges.

Figure 2 shows the surface morphology of the GeSn alloy sample with nominal coverage similar to that shown in Fig. 1, but annealed *in situ* at 150°C for ~ 17 h. While the overall morphological features of the surface are similar to the other samples, the total length and width of the trenches/ridges as well as their fractional coverage is significantly larger than the comparable sample prior to the anneal (e.g., Fig. 1). The ridge height, however, appears to have decreased slightly in comparison with the as-grown films.

Figure 3 shows an AFM image of a ~ 15 nm thick GeSn thin film where the initial stages of track formation are apparent in some regions of the wafer. It is noted

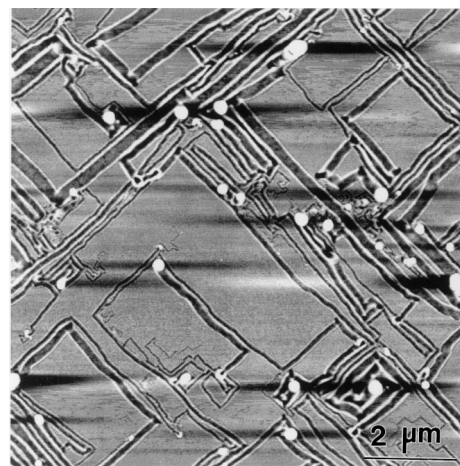


FIG. 2. AFM image ($10 \mu\text{m} \times 10 \mu\text{m}$, height mode) of the surface morphology of a GeSn alloy after 17 h of *in situ* anneal. Notice the increased coverage of the surface with long trenches/ridges.

that the trenches/tracks appear to have been initiated by a single large island separating into two islands, one typically smaller in height than the other. The trench length subsequently increases with an “effective” lateral motion of one or both of these islands. It is important to point out that in the large number of images collected from several samples, we have rarely observed a trench/ridge without an accompanying island. However, the reverse situation where an island has no apparent trench has been seen in some areas of the samples, such as in Fig. 3.

Figure 4(a) shows a plan-view TEM image (taken under a two-beam $\langle 220 \rangle$ dark-field condition) of one of these tracks. The nature of the contrast near the tracks is indicative of a weak epitaxial strain. It is confirmed from the diffraction pattern that the trenches run along $\langle 100 \rangle$ directions. Figure 4(b) shows a cross-sectional view of a

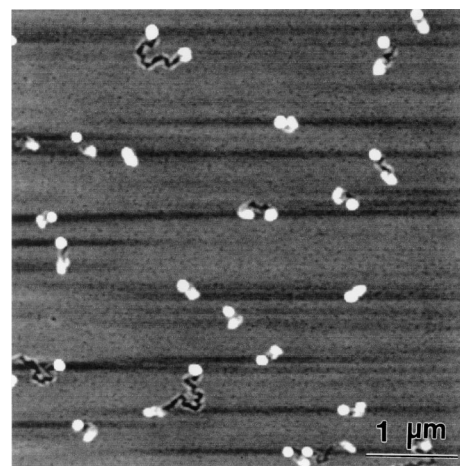


FIG. 3. AFM image ($5 \mu\text{m} \times 5 \mu\text{m}$, height mode) showing surface morphology of an as-grown GeSn sample showing the initial stages of trench formation. Note a few large islands separating into two smaller islands before the initiation of the trenches.

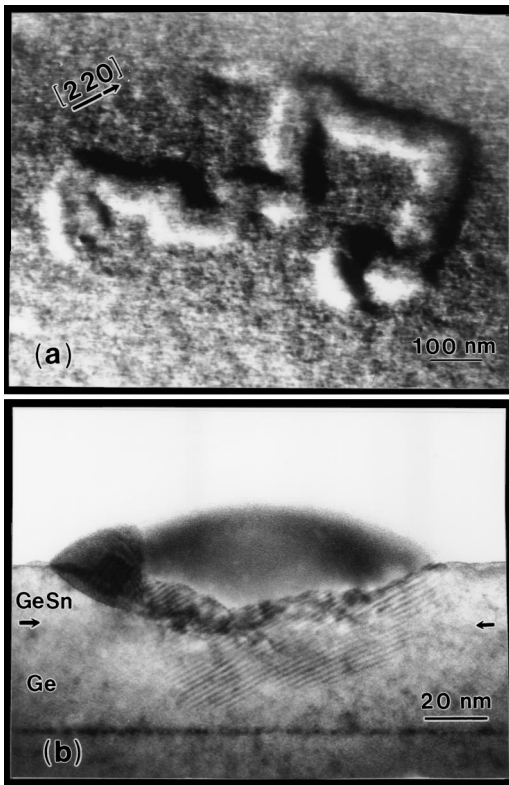


FIG. 4. (a) Plan-view TEM image of a trench. Notice the weak strain contrast and lack of defects within the trench. (b) Cross-sectional TEM view of a large Sn island. Note the interaction volume in this island.

large Sn island. It is clearly seen from the oval shape of the island that some interdiffusion and possibly melting of the film has taken place underneath the island. The Sn island appears asymmetric, with one edge of the island showing moiré fringes indicative of either a different phase or crystallographic misalignment.

Microanalysis using energy dispersive x-ray spectroscopy in a scanning electron microscope indicated that the large islands were Sn-rich while the ridges were indistinguishable from the Ge substrate signal. Further confirmation that the large islands are Sn-rich and the ridges are Ge-rich come from an experiment involving selective chemical etching of Sn.

Limited statistical analyses were performed to get a better understanding of the microstructural changes. The height of the two types of islands (at the two ends of a given trench) was plotted as a function of the total trench length, and is shown in Fig. 5. It is observed that the height of the larger island *increases* with the trench length while the height of the smaller island *decreases* slightly with the trench length. The dependence of the island diameter on the trench length (not shown) is similar. This indicates that the formation of trenches may be linked to the growth of large Sn islands.

Continued growth of the Ge-Sn alloy to form thicker films (~ 60 nm thick) leads to a surface morphology typified by Fig. 6. The AFM image shows a surface with

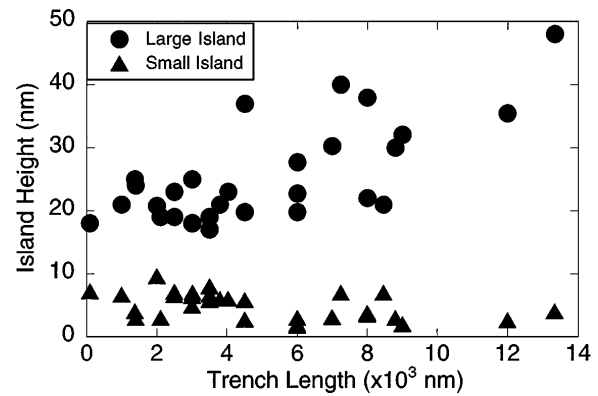


FIG. 5. Plot of the island height as a function of the trench length. The larger islands appear to get larger with trench length, while the smaller islands reduce in height slightly.

domains of parallel trenches (and ridges). The dimensions of the trenches, ridges, and islands have increased with the growth of thicker films.

We begin discussion by recalling the equilibrium phase diagram of the Ge-Sn system. (While an epitaxial phase diagram [8] would be more appropriate, the bulk phase diagram is used in this discussion.) The equilibrium solid solubility of Sn in Ge is $\ll 1$ at. % while the solubility of Ge in Sn is negligible [9]. Consequently, the nominal Ge-Sn alloys used in our studies are likely to be supersaturated with Sn. Furthermore, alloys of Ge-Sn have a larger lattice parameter than Ge; as a result coherent GeSn films will be compressively strained on the Ge substrate. Our substrate temperatures are nominally ~ 150 °C as measured by a thermocouple placed behind the Mo-sample holder on which the substrates are mounted. The errors in the absolute temperature could be as high as ± 25 °C, which indicates that the surface could be close to the melting point of Sn (232 °C).

Based on the observations described earlier, we propose the following model to explain the morphological

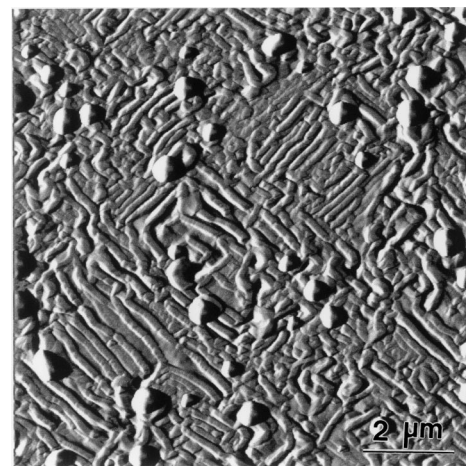


FIG. 6. AFM image ($10 \mu\text{m} \times 10 \mu\text{m}$, amplitude mode) showing the formation of domains of trenches and islands in a ~ 60 nm thick GeSn alloy.

features observed in our experiments. At the initial stages of Ge-Sn deposition, the surface undergoes Sn-induced changes in reconstructions. Based on our RHEED observations and reports from the literature, it is clear that Sn segregates to the surface [10,11]. A few monolayers accumulate before incorporation of Sn in Ge may take place within the thin film [10]. The surface is relatively smooth at this point as confirmed by AFM analysis of ~ 2 nm thick films.

Continued growth leads to the nucleation of a low density of Sn islands on the surface. These Sn islands are likely to be either liquid or have a liquid film on their surfaces. Since the fraction of Ge in the nominal alloy is very high, a significant amount of Ge must get trapped inside the Sn islands due to deposition from the vapor, as well as from the interaction of the Sn island in contact with the Ge-Sn film. The Ge atoms agglomerate and separate from the parent Sn island as seen in Fig. 3. The Ge-rich island so formed is likely to have a composition closer to the equilibrium Ge-Sn alloy and would be more strain relaxed in comparison with the nominal alloy film. The removal of supersaturated Sn and Ge in the alloy film from within the interaction volume creates a trench on the strained surface.

It is now well understood that the presence of a trench (or island) reduces the strain in a coherent epitaxial film, due to the lattice relaxation at the edge of the trench (or island) [5–7]. Further evidence for the strain relaxation comes from the fact that the trenches are formed along the elastically soft $\langle 100 \rangle$ directions [7], and from the strain contrast seen in plan-view TEM images. The situation can then be viewed as follows. One side of the large Sn island is in contact with a GeSn alloy that is partially strain relaxed at the trench edge and on the ridge. On all other sides, the Sn island is in contact with a coherently strained SnGe alloy. The Ge atoms are therefore at a higher chemical potential in the strained film compared with the relaxed regions. This chemical potential difference sets up a diffusional flux of Ge towards the relaxed SnGe alloy near the pit. The Ge precipitates out at the other end of the Sn island forming the Ge-rich ridge. The mass transport of Ge across the Sn island causes a net migration of the Sn island in a $\langle 100 \rangle$ direction creating the trenches and ridges. In the process, the Sn island grows by collecting Sn from the GeSn film and precipitating out the Ge leading to phase separation. The reduction in size of the Ge-rich island at the other end of the trench can be explained on the basis of capillarity driven smoothing of the island. This is also consistent with the disappearance of small islands from the trench (and reduction in ridge height) in the annealing experiments.

The mechanism of migration of Sn islands and precipitation of Ge appears to be similar in nature to the migration of grain boundaries (or liquid films) in conjunction with cellular precipitation in metallurgical systems [12,13]. In such cases, while the migration of grain

boundaries almost always increases the grain boundary area (and thus the total interfacial energy), all the solute atoms in the volume swept by the migrating boundary have the opportunity to diffuse to the stable phase along a short circuit diffusion path. As a result the precipitation rate (relaxation to equilibrium) is increased manyfold [13]. Migration of In or Sn droplets driven by free-energy gain across an amorphous-crystalline interface have also been reported [14].

In summary, we have observed the self-organized formation of trenches and ridges by the effective lateral migration of Sn islands on the surface. The mechanism for this motion is suggested to be a diffusional flux of Ge to regions of lower chemical potential on one side of the Sn island. The microstructural evolution may be a kinetic pathway for phase separation of Ge and Sn from the metastable Ge-Sn alloy. By controlling the size scales and pattern distribution, the observed phenomenon could be used in the high-throughput fabrication of quantum wires (Ge ridges) and in nanolithography (trenches). This mechanism may be a common feature of other epitaxially strained alloy thin films.

We wish to acknowledge invaluable discussions with Professor T.H. Courtney and Professor D.J. Swenson. Financial support for this work was provided in part by ONR (N00014-96-1-0793), NSF (DMR 9624456), and DARPA-Ultra Nanoelectronics (F49620-96-1-0313).

*Electronic address: mohan@mtu.edu

- [1] O. Gurdal *et al.*, Appl. Phys. Lett. **67**, 956 (1995).
- [2] See, for example, E. A. Fitzgerald, Mater. Sci. Rep. **7**, 87 (1991).
- [3] D. J. Eaglesham and M. Cerullo, Phys. Rev. Lett. **64**, 1943 (1990); S. Guha, A. Madhukar, and K. C. Rajkumar, Appl. Phys. Lett. **57**, 2110 (1990).
- [4] Y-W. Mo *et al.*, Phys. Rev. Lett. **65**, 1020 (1990).
- [5] D. J. Srolovitz, Acta Metall. **37**, 621 (1989).
- [6] J. Tersoff and F. K. LeGoues, Phys. Rev. Lett. **72**, 3570 (1994).
- [7] V. A. Shchukin *et al.*, Phys. Rev. Lett. **75**, 2968 (1995); D. E. Jesson *et al.*, Phys. Rev. Lett. **77**, 1330 (1996).
- [8] I. P. Ipatova, V. G. Malyshekin, and V. A. Shchukin, J. Appl. Phys. **74**, 7198 (1993); D. M. Wood and A. Zunger, Phys. Rev. B **40**, 4062 (1989).
- [9] T. B. Massalski, *Binary Alloy Phase Diagrams* (American Society for Metals, Metals Park, OH, 1986), Vol. 2.
- [10] W. Wegscheider *et al.*, J. Cryst. Growth **123**, 75 (1992).
- [11] P. R. Pukite, A. Harwit, and S. S. Iyer, Appl. Phys. Lett. **54**, 2142 (1989).
- [12] See, for example, D. A. Porter and K. E. Easterling, *Phase Transformations in Metals and Alloys* (Van Nostrand Reinhold, Berkshire, 1981).
- [13] See, for example, S. A. Hackney and F. S. Biancaniello, Scr. Metall. **21**, 371 (1987); C. A. Handwerker *et al.*, in *Diffusion in Solids: Recent Developments*, edited by M. D. Dayananda and G. E. Murch (Metallurgical Society, Warrendale, PA, 1986).
- [14] E. Nygren *et al.*, Mater. Res. Soc. Symp. Proc. **100**, 405 (1988); O. Hellman, J. Appl. Phys. **76**, 3818 (1994).